

Numerical Simulation of Hydrodynamic-Based Microfluidic Device for Single Cell Trapping

Amelia Ahmad Khalili, Mohd Ariffanan Mohd Basri, Salma Binslem, and Mohd Ridzuan Ahmad

Abstract— Single cell analysis has become the interest of a wide range of biological and biomedical engineering research. It could provide precise information of the individual cells which leads to important knowledge regarding human's diseases. Many attempts have been done to perform single cell analysis which require the isolation of individual cells before further manipulation could be carried out. Recently, microfluidic has been widely used for cell trapping and single cell analysis such as mechanical and electrical detection. Hydrodynamic trapping could be applied in the microfluidic device to trap a single cell thus providing platform for further cell characterization. This paper presents a finite element model for single cell trapping using hydrodynamic concept. The proposed microfluidic device consists of two parallel microchannels (main channel and trapping channel). Fluid's flow rates are optimized by performing microchannel geometrical size manipulation to isolate a $5\ \mu\text{m}$ yeast cell. The analysis was carried out using finite element ABAQUS-FEA software. The optimized $Rh_{\text{Main}}/Rh_{\text{Trap}}$ ratio was 3.5 and above for successful trapping.

I. INTRODUCTION

Nowadays, the Lab on a Chip (LOC) or Micro Total Analysis Systems (μTAS) based on microfluidics has attracted the researchers attention in biotechnological and biomedical engineering areas. The arises of the interest is due to the utilization of these devices in a broad range of biological and biomedical application areas including genomics, enzymatic analysis, diseases diagnosis, cell treatment, drug screening, single cell analysis, drug delivery etc. In cellular biology, single cell analysis refers to the study of individual cells isolated from tissues in multi-cellular organisms. Conventionally, cell analyses are conducted with large populations of cells and data measurement can only represent the average values summed over the responses of many cells. Therefore, single cell analysis is important to obtain more precise information and to reveal the properties of individual cells and cell-to-cell differences [1].

In order to perform single cell analysis in microfluidic devices, trapping of a single cell is necessary. Variety of

techniques have been employed to trap an individual cell. For example, microwell-based [2–4], dielectrophoresis-based [5–7] and hydrodynamic-based [8–11] microfluidic devices for single cell trapping have been developed in response to an increasing demand for simple yet reliable tools for high-throughput cell manipulation at the single cell level. In microwell-based platforms, designing the microwells with a precise geometry is required to achieve a high trapping efficiency [2]. Dielectrophoresis-based cell trapping applied a non-uniform AC field to manipulate polarized particles in suspension and is an effective technique to efficiently manipulate single cell. However, it appears to damage the trapped cells, thus affecting the cell proliferation. Hydrodynamic trapping uses the altered fluidic resistance created by microstructures on a fluid path, such as sieve-like traps [8-9] or small trapping sites [10–13] to control the movement of cells in a microchannel. For the straight or serpentine-shaped channels with trapping sites, the fluidic resistances of these channels are carefully calculated so that the fluid and cells in the main channel will preferentially flow into the trapping sites when they are empty, but bypass them when they are occupied with a cell. The main challenge in hydrodynamic trapping is that it requires a precise microfluidic control of multiple streams. In addition, further investigation and optimization on cells trapping efficiencies are still requested [14].

In this work, a proof of concept demonstration of a cell positioning platform using hydrodynamic manipulation to trap a single cell is presented. The proposed microfluidic device consists of two parallel microchannels (main channel and trapping channel). The flow rates in the microfluidic devices are optimized by performing microchannel geometrical size optimization. Numerical simulations are conducted to evaluate the cells trapping efficiencies for a variety of geometrical parameters.

II. THE IDEA AND CONCEPT OF THE MODEL

The concept of hydrodynamic trapping was originally proposed by Tan et al.[12] where the microchannels are designed such that: (a) the trapping channel has a lower flow resistance than that of the by-pass channel when a trapping site is empty, and will make the beads/cells flow into the trapping stream and directed into the trap; (b) when a bead/cell was trapped, it will act as a plug and will increase the flow resistance along the trapping channel drastically; and (c) the main flow will change from the trap channel to the by-pass channel (main channel in our model) and the next beads/cells will be directed to the by-pass stream, pass by the filled trapping site[15]. Darcy-Weisbach equation is used to determine the pressure drop or pressure difference in a

Research supported by Ministry of Higher Education Malaysia and Universiti Teknologi Malaysia.

A. A. Khalili, is with the Dept. of Control and Mechatronic Engineering, Faculty of Electrical Engineering, Universiti Teknologi Malaysia, 81310 Skudai, Johor, Malaysia (e-mail: amelia.ahmadkhalili@gmail.com).

M. A. M. Basri, is with the Dept. of Control and Mechatronic Engineering, Faculty of Electrical Engineering, Universiti Teknologi Malaysia, 81310 Skudai, Johor, Malaysia

M. R. Ahmad, is with the Dept. of Control and Mechatronic Engineering, Faculty of Electrical Engineering, Universiti Teknologi Malaysia, 81310 Skudai, Johor and Institute of Ibnu Sina, Universiti Teknologi Malaysia, 81310 Skudai, Johor, Malaysia (corresponding author e-mail: ridzuan@fke.utm).

microchannel and solving the continuity and momentum equations for the Hagen-Poiseuille flow problem.

From Hagen-Poiseuille's equation, the flow rate (Q) can be defined as following equation:

$$\Delta P = Q \times R_h = Q \times \left(\frac{12\mu L}{WH^3} \right) \quad (1)$$

where ΔP is the pressure drop, R_h is the hydrodynamic flow resistance of the rectangular microchannels, μ is the fluid viscosity, L , H and W are length, height and width of the channel respectively. Considering microchannel acts as a resistive circuit, R_h is analogous to resistance in an electric circuit, this equation is an analogue of Ohm's law ($V = IR$), where ΔP and Q are the analogs of V and I , respectively[16].

Figure 1 shows the schematic explanation of the hydrodynamic trapping concept with R_{Trap} and R_{Main} representing the flow resistance for trapping channel and main channel, respectively. At intersection (Figure 1), the flow is divided into the trap-path and the main-path. Yellow circle denotes the yeast cells to be trapped. The flow rates of the trap-path (Q_{Trap}) and the main-path (Q_{Main}) are distributed depending on the corresponding flow resistances. By using a relationship of $A = W \times H$ and $P = 2(W + H)$, the hydrodynamic flow resistance can be formulated in the following equation:

$$R_h = \frac{C\mu LP^2}{A^3} \quad (2)$$

where C denotes a constant that depends on the aspect ratio (H/W), A is the cross-sectional area and P is the perimeter of the channel. The flow rate ratio between trap path and main path can be modelled as given in equation (3), approximating that the pressure drop across main path and trap path are same [17]. For the trap to work, the flow rate along trap path must be greater than that of main path ($Q_{Trap} > Q_{Main}$).

$$\frac{Q_{Trap}}{Q_{Main}} = \left(\frac{L_M}{L_T} \right) \cdot \left(\frac{W_M + H_M}{W_T + H_T} \right)^2 \cdot \left(\frac{W_T H_T}{W_M H_M} \right)^3 \quad (3)$$

The flow rate ratio at each bifurcation could be determined by controlling the hydrodynamic resistance ratio between the main channel and trap channel. The flow rate of whole fluid at the inlet could be assumed as an electric current source. Outlet which leads to the atmospheric pressure could be assumed as grounds.

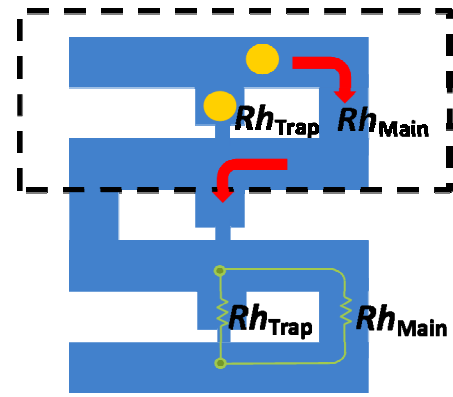


Figure 1 Simple schematic of single cell trapping channel with the hydrodynamic resistance.

Inspired by the concept proposed by Tan and Takeuchi (2007), we developed a finite element single cell trapping model to verify the concept using numerical simulation. In the model, cells will be introduced into the device through the inlet with appropriate flow rate and directed to the trap channel by designing appropriate main channel's length. The main channel's length will be optimized to get the appropriate R_h ratio that leads to successful trapping. The excess and remaining cells will be directed out through the channel's outlet by injecting cell's culture medium. The appropriate channel's geometry to trap single yeast cell in the specified design was studied. The finite element single cell trapping model was focusing only on a single trap channel (refer dashed box in figure 1) for geometry optimization due to the complexity and high processing time required for the analysis.

III. SIMULATION SETUP

The analysis was carried out using finite element ABAQUS-FEA analysis software which able to perform multi-physics analysis. Initially, the simulation analysis was carried out using the parameters in micro dimension properties. However due to time consumed for the simulation to converge is too long (data not shown), the parameters was appropriately scaled into meter dimension with the ratio of 1 m is proportional to 1 μm . The advantage of dimension scaling is that a simulation works could be carried out in a reasonable simulation times[18]. The approach to represents a nano scale model by giving nanometer dimensions to the geometry and using the material property values identical to the scale model suffers from two major drawbacks. Firstly, the simulation will face a very small incremental time steps which would make real time simulation prohibitively expensive if not impossible and secondly, using properties with nanometer dimensions will create numerical issues in finite element programs [18].

The fluid microchannel was modeled as 3D Eulerian explicit EC3DR and an 8-node linear Eulerian brick element part assigned with water properties (density, equation of state, viscosity). Figure 2(A-B) shows the different parts involved in the model; an eulerian part with the fluid channel and a three dimension (3D) deformable part of the sphere-shaped elastic yeast cell model (5 μm in diameter) and figure

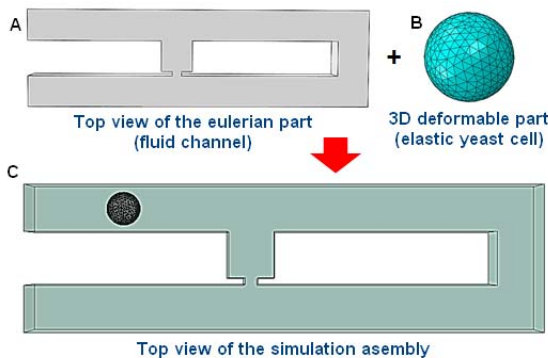
2C shows the assembly setup with a yeast cell positioned in the main channel, near the channel's inlet (left).

The microchannel consists of two channels; the main channel (loop channel) with the width and depth of $7\text{ }\mu\text{m}$ and total length of the main path (refer figure 1 on the path of Rh_{Main}) varies from $46\text{ }\mu\text{m}$ to $268\text{ }\mu\text{m}$ and a trap channel with $7\text{ }\mu\text{m}$ of length, width and depth. There is one rectangular trap hole placed at the centre edge of the trap channel with the dimension of $1\text{ }\mu\text{m}$ and $7\text{ }\mu\text{m}$ of length and height, respectively. The height of suction hole is a variable ranging from $1.5 - 2.0\text{ }\mu\text{m}$, with $2.0\text{ }\mu\text{m}$ was set as the height for the initial simulation analysis.

A sphere-shaped yeast cell ($5\text{ }\mu\text{m}$ in diameter) was model as an elastic 3D standard solid deformable C3D8R and an 8-node linear brick 3D part with the yeast properties (Young's Modulus, Poisson's Ratio, density, etc.) obtained from literature [19–26]. The developed parts were assembled to develop the finite element model of the proposed system (Figure 2C). The fluid channel and cell was meshed using hexahedron and tetrahedron mesh types, respectively. Total mesh total elements ranged from 10627 to 22 485 elements. No-inflow and non-reflecting outflow Eulerian boundary conditions were applied to the channel's wall. Inflow velocity of $0.5\text{ }\mu\text{m s}^{-1}$ was applied to the inlet and atmosphere pressure was applied to the outlet of the channel for all the models analyzed. Various main channel's length ranging from $46\text{ }\mu\text{m}$ to 268 and trap hole's width ranging from $1.5\text{ }\mu\text{m}$ to $2.0\text{ }\mu\text{m}$ were applied to produce the appropriate Rh for single cell trapping analysis. The initial position of cell was fixed to the same position (distance between cell and trap channel) for all the models used. Interaction between objects and water was set as general contact with rough tangential behaviour and the interaction between cell surface and channel's wall was set as frictionless.

IV. RESULTS AND DISCUSSION

According to the hydrodynamic trapping concept proposed by Tan and Takeuchi (2007), single cell/particle trapping should able to be achieved when $Q_{\text{Trap}}/Q_{\text{Main}}$ ratio is above 1 [12]. The finite element analysis was carried out to verify the concept and geometry manipulation optimization was performed to achieve appropriate channel's dimension to trap a $5\text{ }\mu\text{m}$ single yeast cell. The main channel's length was



manipulated to develop the hydrodynamic ratio between main channel to the trap channel ($Rh_{\text{Main}}/Rh_{\text{Trap}}$) ranging from 1 to 6. Increasing the $Rh_{\text{Main}}/Rh_{\text{Trap}}$ is proportional with the increase in main channel's (loop path) length. Abaqus FEA uses the Navier-Stokes equation in solving the fluid motion. Initially, the trap hole's width of $2\text{ }\mu\text{m}$ was used for the analysis and yeast cell model was found able to be trapped when $Rh_{\text{Main}}/Rh_{\text{Trap}}$ of 3.5 and higher was used (figure 3C-3D). Results obtained showed that the concept didn't work for the model with $Rh_{\text{Main}}/Rh_{\text{Trap}}$ of $1.0 - 3.0$ and the cell movement was found not directed to the trap channel but moved passed through the trap channel (refer figure 3(A-B) for $Rh_{\text{Main}}/Rh_{\text{Trap}}$ model of 1.5 and 2.5, results for $Rh_{\text{Main}}/Rh_{\text{Trap}}$ model of 1.0 and 2.0 are not shown). Subsequent simulation was carried out using the model with trap hole's width $1.5\text{ }\mu\text{m}$ and similar results were obtained when the trap hole's width was decrease to $1.5\text{ }\mu\text{m}$ (refer table 1). The hydrodynamic concept works accordingly when $Rh_{\text{Main}}/Rh_{\text{Trap}}$ is 3.5 and above and the single yeast cell model able to be directed towards the trap channel with the fluid stream.

Streamline plots of model with suction hole's width of $2\text{ }\mu\text{m}$ were obtained for $Rh_{\text{Main}}/Rh_{\text{Trap}}$ ratio of 1.5 to 4.5 are shown in figure 5. The streamline velocity field for $Rh_{\text{Main}}/Rh_{\text{Trap}}$ 3.5 and above (figure 4 C and D) show that the flow diverged from main channel to the trap channel and all the streamlines were directed towards the trap channel. In contrast to the $Rh_{\text{Main}}/Rh_{\text{Trap}}$ below 3.5 (figure 4A- 4B), the velocity streamlines were not fully directed to the trap channel as portions of the streamlines were directed pass through the main channel and towards the trap channel. The velocity streamlines obtained were not fully focusing towards trapping channel and unable to produce enough force to trap the cell into trapping channel. Colour contours in the results show different velocity from low (dark blue) to high (light grey).

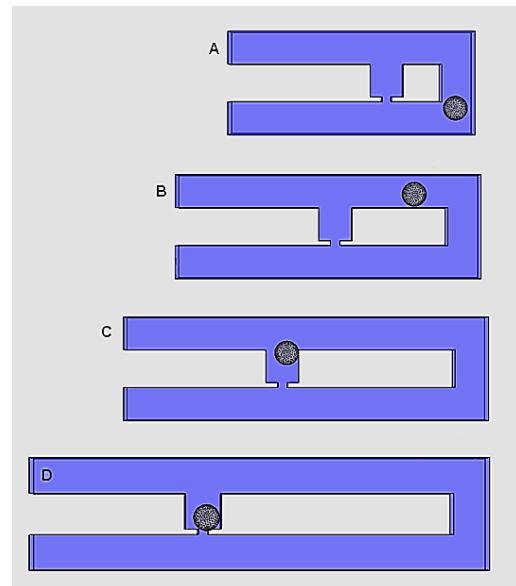


Table 1: Simulation findings for single cell trapping for different trap hole's width.

Ratio of Rh_{Main}/Rh_{Trap}	Ability to trap cell	
	Trap hole's W : 1.5 μm	Trap hole's W : 2.0 μm
1.0	x	x
1.5	x	x
2.0	x	x
2.5	x	x
3.0	x	x
3.5	yes	yes
4.5	yes	yes
5.0	yes	yes
5.5	yes	yes
6.0	yes	yes

Figure 5 shows the fluid's velocity distribution before cell reach the trap channel (simulation time 14 s) for single cell trapping model (trapping hole's width 2 μm) with Rh_{Main}/Rh_{Trap} between 1.5 to 4.5. Results show that the main channel's (loop path) fluid velocity of the single cell trapping model with Rh_{Main}/Rh_{Trap} of 1.5 and 2.5 (figure 5A-B) is high compared to the trap channel's fluid velocity. Therefore the main stream will direct the yeast cell to flow to the main channel's path and bypass the trap channel. In contrast to the model with Rh_{Main}/Rh_{Trap} of 3.5 and 4.5 (figure 5C-D), the fluid's velocity distribution from the trap hole to the trap channel is higher compared to the fluid's velocity in the main channel. These show that the trap channel produced lower hydrodynamic resistance than the main channel and the main stream will direct the yeast cell into the trap channel (refer figure 4C-D). However, results show that both model with Rh_{Main}/Rh_{Trap} of 3.5 and 4.5 produced almost the same fluid's velocity pattern that will produced appropriate pressure drop for the cell to be trapped. Similar results were observed with the single cell trapping model with trapping hole's width 2 μm (data not shown).

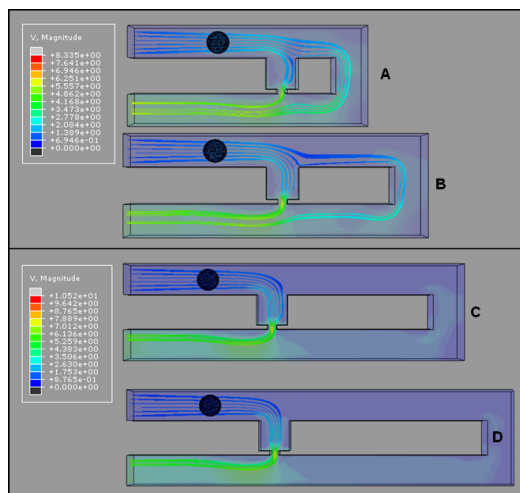


Figure 4: Streamline velocity field of the single cell trapping model (top view) with trapping hole's width of 2 μm for Rh_{Main}/Rh_{Trap} of (A) 1.5 (B) 2.5 (C) 3.5 (D) 4.5.

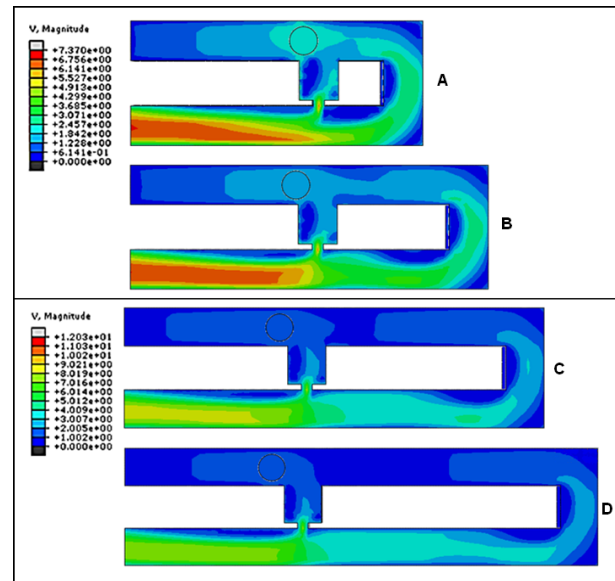


Figure 5: Velocity of fluid before cell trapping for single cell trapping model with trapping hole's width of 2 μm for Rh_{Main}/Rh_{Trap} of (A) 1.5 (B) 2.5 (C) 3.5 (D) 4.5. Round structure inside the channel represent the yeast cell model.

From the simulation results, it was found that the single cell trapping model with Rh_{Main}/Rh_{Trap} below 3.5 failed to trap the yeast cell model and trapping was successful when the Rh_{Main}/Rh_{Trap} is above the value of 3.5 (refer table 1). However, there are variations in the complete cell trapping time (time when the cell touch the surface of trap channel) obtained between different Rh_{Main}/Rh_{Trap} ratio. Higher ratio requires shorter time for trapping process compared to the lower ratio. Graph in figure 6 shows the results of trapping time for the single cell trapping model with trapping hole's width 1.5 μm and 2.0 μm for Rh_{Main}/Rh_{Trap} from 3.5 to 6.0. From the graph, it shows that the trapping time decreased with the increasing of Rh_{Main}/Rh_{Trap} . This is probably because higher Rh_{Main}/Rh_{Trap} able to perform velocity distribution (from suction hole's to the whole area of trap channel) in a shorter time compared to the lower Rh_{Main}/Rh_{Trap} . A greater Rh_{Main}/Rh_{Trap} ratio was found could provide a lower hydrodynamic resistance in the trap channel and could transfer the fluid at a faster rate. The velocity distribution produced different pressure from main channel to the trap hole, making the flow resistance inside the trapping channel lower than the main channel. Therefore, together with the fluid, cell will flow to the lower flow resistance area and be trapped. Bigger suction hole's height (2.0 μm) able to produced shorter trapping time compared to the smaller height (1.5 μm). Both design with suction hole's width of 1.5 μm and 2.0 μm able to obey the hydrodynamic trapping concept as cell was found able to be trap into the trap channel.

This study provides a finite element model for single cell trapping for a yeast cell model. Trap channel's was designed to specifically trap a 5 μm yeast cell via hydrodynamic resistance manipulation using a trapping hole placed in the edge of the trap channel. The channel's geometry was optimized to produce appropriate ratio of hydrodynamic resistance between the trap channel and the main channel (loop path). The single cell trapping finite element model was

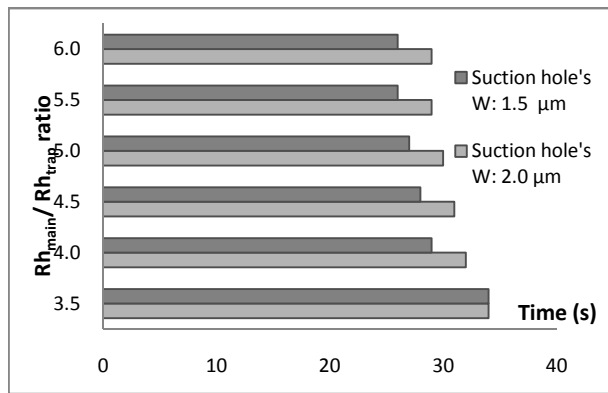


Figure 6: Simulation results of cell trapping time for different Rh_{Main}/Rh_{Trap} from 3.5 to 6.0 for single cell trapping model with trapping hole's width of 1.5 and 2.0 μm .

found able to trap a single yeast cell into the trap channel with optimized main channel's geometry and appropriate Rh_{Main}/Rh_{Trap} .

Single cell trapping channel is important in providing a good platform for cell manipulation in studying the biological, biophysical or biomedical aspect of the cells. Optimization of the trap channel geometry able to be carried out by analyzing the fluid's (water) velocity distribution and by observing the success of cell trapping into trap hole in the analyzed model. Suction hole's height of 1.5 μm should be chosen to carry out single cell analysis because the size is not too big and enough to trap single cell and to minimize access stress from executing the trapped cell. However, the size of suction hole to be chosen is dependent on the type of cell and type of experiment or analysis and how will it be performed.

V. CONCLUSION

This study presents the finite element model of single cell trapping inside microfluidic channel. This single cell trapping system able to be constructed using Abaqus-FEA™ software. The single cell trapping model able to follow the hydrodynamic resistance trapping concept. The appropriate Rh_{Main}/Rh_{Trap} to perform cell trapping using hydrodynamic resistance concept is the ratio value above than 3.5. A 5 μm yeast cell model able to be trapped inside a trap channel with height, width and length of 7 μm by manipulating the main channel's length of the model with trap hole's width 1.5 and 2.0 μm which situated at the centre edge of the trap channel. This cell trapping model able to isolate an individual yeast cell inside fluidic environment thus provide a platform to further study the mechanical or biological behaviour of single cell. Single cell manipulation such as chemical and biophysical treatments and also mechanical characterization could be performed inside the microfluidic channel using this system.

ACKNOWLEDGMENT

The research was supported by Ministry of Education Malaysia (grant nos. 4L640 and 4F351) and Universiti Teknologi Malaysia (grant nos. 02G46, 03H82 and 03H80).

REFERENCES

- [1] R. M. Johann, "Cell trapping in microfluidic chips," *Analytical and bioanalytical chemistry*, vol. 385, no. 3, pp. 408–12, Jun. 2006.
- [2] J. R. Rettig and A. Folch, "Large-Scale Single-Cell Trapping And Imaging Using Microwell Arrays," vol. 77, no. 17, pp. 5628–5634, 2005.
- [3] J. Tang, R. Peng, and J. Ding, "The regulation of stem cell differentiation by cell-cell contact on micropatterned material surfaces," *Biomaterials*, vol. 31, no. 9, pp. 2470–2476, Mar. 2010.
- [4] J. Doh, M. Kim, and M. F. Krummel, "Cell-laden microwells for the study of multicellularity in lymphocyte fate decisions," *Biomaterials*, vol. 31, no. 12, pp. 3422–3428, Apr. 2010.
- [5] J. Voldman, M. L. Gray, M. Toner, and M. A. Schmidt, "A Microfabrication-Based Dynamic Array Cytometer," *Analytical Chemistry*, vol. 74, no. 16, pp. 3984–3990, Jul. 2002.
- [6] R. S. Thomas, H. Morgan, and N. G. Green, "Negative DEP traps for single cell immobilisation," *Lab on a Chip*, vol. 9, no. 11, pp. 1534–1540, 2009.
- [7] D. S. Gray, J. L. Tan, J. Voldman, and C. S. Chen, "Dielectrophoretic registration of living cells to a microelectrode array," *Biosensors and Bioelectronics*, vol. 19, no. 7, pp. 771–780, Feb. 2004.
- [8] D. Di Carlo, N. Aghdam, and L. P. Lee, "Single-Cell Enzyme Concentrations, Kinetics, and Inhibition Analysis Using High-Density Hydrodynamic Cell Isolation Arrays," vol. 78, no. 14, pp. 4925–4930, 2006.
- [9] A. M. Skelley, O. Kirak, H. Suh, R. Jaenisch, and J. Voldman, "Microfluidic control of cell pairing and fusion," *Nat Meth*, vol. 6, no. 2, pp. 147–152, Feb. 2009.
- [10] P. J. Lee, P. J. Hung, R. Shaw, L. Jan, and L. P. Lee, "Microfluidic application-specific integrated device for monitoring direct cell-cell communication via gap junctions between individual cell pairs," *Applied Physics Letters*, vol. 86, no. 22, p. 223902, 2005.
- [11] J.-P. Frimat, M. Becker, Y.-Y. Chiang, U. Marggraf, D. Janasek, J. G. Hengstler, J. Franzke, and J. West, "A microfluidic array with cellular valving for single cell co-culture," *Lab on a chip*, vol. 11, no. 2, pp. 231–7, Jan. 2011.
- [12] W.-H. Tan and S. Takeuchi, "A trap-and-release integrated microfluidic system for dynamic microarray applications," *Proceedings of the National Academy of Sciences of the United States of America*, vol. 104, no. 4, pp. 1146–51, Jan. 2007.
- [13] K. Chung, C. A. Rivet, M. L. Kemp, H. Lu, and U. States, "Imaging Single-Cell Signaling Dynamics with a Deterministic High-Density Single-Cell Trap Array," *Analytical chemistry*, pp. 7044–7052, 2011.
- [14] S. Kobel, A. Valero, J. Latt, P. Renaud, and M. Lutolf, "Optimization of microfluidic single cell trapping for long-term

on-chip culture,” *Lab on a chip*, vol. 10, no. 7, pp. 857–63, May 2010.

- [15] T. Teshima, H. Ishihara, K. Iwai, A. Adachi, and S. Takeuchi, “A dynamic microarray device for paired bead-based analysis,” *Lab on a chip*, vol. 10, no. 18, pp. 2443–8, Sep. 2010.
- [16] Z. Tang, Y. Akiyama, K. Itoga, J. Kobayashi, M. Yamato, and T. Okano, “Shear stress-dependent cell detachment from temperature-responsive cell culture surfaces in a microfluidic device,” *Biomaterials*, vol. 33, no. 30, pp. 7405–11, Oct. 2012.
- [17] I. Kumano, K. Hosoda, H. Suzuki, K. Hirata, and T. Yomo, “Hydrodynamic trapping of *Tetrahymena thermophila* for the long-term monitoring of cell behaviors,” *Lab on a chip*, vol. 12, no. 18, pp. 3451–7, Sep. 2012.
- [18] G. Thiagarajan, K. Deshmukh, Y. Wang, A. Misra, J. L. Katz, and P. Spencer, “Nano finite element modeling of the mechanical behavior of biocomposites using multi-scale (virtual internal bond) material models,” *Journal of Biomedical Materials Research Part A*, vol. 83, no. 2, pp. 332–344, 2007.
- [19] T. Gervais, J. El-Ali, A. Günther, and K. F. Jensen, “Flow-induced deformation of shallow microfluidic channels,” *Lab on a chip*, vol. 6, no. 4, pp. 500–7, Apr. 2006.
- [20] A. K. Bryan, A. Goranov, A. Amon, and S. R. Manalis, “Measurement of mass, density, and volume during the cell cycle of yeast,” *Proceedings of the National Academy of Sciences of the United States of America*, vol. 107, no. 3, pp. 999–1004, Jan. 2010.
- [21] M. R. Ahmad, M. Nakajima, S. Kojima, M. Homma, and T. Fukuda, “The effects of cell sizes, environmental conditions, and growth phases on the strength of individual W303 yeast cells inside ESEM,” *IEEE transactions on nanobioscience*, vol. 7, no. 3, pp. 185–93, Sep. 2008.
- [22] A. E. Smith, Z. Zhang, C. R. Thomas, K. E. Moxham, and A. P. Middelberg, “The Mechanical Properties of *Saccharomyces Cerevisiae*,” *Proceedings of the National Academy of Sciences of the United States of America*, vol. 97, no. 18, pp. 9871–4, Aug. 2000.
- [23] J. D. Stenson, C. R. Thomas, and P. Hartley, “Modelling the mechanical properties of yeast cells,” *Chemical Engineering Science*, vol. 64, no. 8, pp. 1892–1903, Apr. 2009.
- [24] J. D. Stenson, P. Hartley, C. Wang, and C. R. Thomas, “Determining the mechanical properties of yeast cell walls,” *Biotechnology progress*, vol. 27, no. 2, pp. 505–12, 2011.
- [25] T. P. Burg, M. Godin, S. M. Knudsen, W. Shen, G. Carlson, J. S. Foster, K. Babcock, and S. R. Manalis, “Weighing of biomolecules, single cells and single nanoparticles in fluid,” *Nature*, vol. 446, no. 7139, pp. 1066–9, May 2007.
- [26] J. Lee, R. Chunara, W. Shen, K. Payer, K. Babcock, T. P. Burg, and S. R. Manalis, “Suspended microchannel resonators with piezoresistive sensors,” *Lab on a chip*, vol. 11, no. 4, pp. 645–51, Mar. 2011.